

Thermal stability and percolation threshold of Ge-Se-Fe glasses

G.Saffarini^{1*}, J.M.Saiter¹, J.Matthiesen²

1: Laboratoire PBM, UMR 6522, LECAP, Institut des Matériaux de Rouen, Faculté des Sciences, Avenue de l'Université BP 12, 76801 Saint Etienne du Rouvray, France

2 : Anorganische Chemie, Universität Osnabrück, D-49069, Osnabrück, Germany

Abstract

The characteristic temperatures such as the glass transition temperature (T_g), the onset temperature of crystallization (T_c) and the melting temperatures, (T_m) have been determined for glasses belonging to the $\text{Ge}_x\text{Se}_{100-x-y}\text{Fe}_y$ ($y=2, 4$ and 6 at%). Differential scanning calorimetry and differential thermal analysis measurements have been used for their determination. These temperatures have been used to evaluate the thermal stability of the investigated glassy alloys using Dietzel (ΔT) and Hruby (H_r) criteria. The variations of ΔT and H_r with the average coordination number, n , have been specified. It is found that both ΔT and H_r exhibit a maximum at $n=2.4$. This observation is a realization of Phillips'-Thorpe threshold where the maximum stability of the network is just obtained if the percolation threshold limit is reached. The overall mean bond energies of the studied compositions have also been calculated and their correlation with the glass transition temperature is discussed

PACS: 61.43.Fs; 65.60.+a.

Keywords: Chalcogenides; Glasses; Thermal stability, Phillips'-Thorpe threshold; Ge-Se-Fe.

* Corresponding author, e-mail: saffarini1@yahoo.com

1. Introduction

Since the discovery of non-oxide semi-conducting chalcogenide glasses five decades ago, they received great attention due to their potential technological applications. However, the early period big boom of interest decreased when it was realized that the first hoped application in TV tubes was not as successful as it was initially projected. In recent years, there has been a resurgence of interest in these materials because of their new promising technological applications which include their use as materials for infrared optical fibers, photoconductors, optoelectronic circuits, optical memories [1-6] and as solid electrolytes [7]. Nevertheless, the technological applications of these materials are usually limited by their physical, mechanical and thermal properties. Therefore, the measurement of the glass transition (T_g), crystallization (T_c) and melting (T_m) temperatures for chalcogenide glasses is of great importance to establish their thermal stability and the useful range of operating temperatures for a particular technological application before the eventual crystallization takes place. Furthermore, wide glass forming regions in these materials offer ample possibilities for controlling the desired thermal property by means of changing the chemical composition.

Because the addition of impurities as a third element has been useful in understanding the thermal properties of chalcogenide glasses, we propose in this work to study the role played by metallic iron on the thermal properties of covalently bonded Ge-Se glasses. To our knowledge, there are few studies on the thermal properties of chalcogenide glasses containing iron. This is probably due to its metallic character which limits the glass forming domain to a maximum of 10 at % of Fe [8]. The aim of the present work is, therefore, to obtain more insight into the thermal stability of the scarcely studied $\text{Ge}_x\text{Se}_{100-x-y}\text{Fe}_y$ ($y=2, 4$ and 6 at%) glasses and also to obtain information on its relationship with the average coordination number.

2. Experimental details

Appropriate amounts of high-purity Ge (99.9999%; ABCR), Se (99.999%; Heraeus) and Fe (99.98%; Strem) were encapsulated in a cylindrical (8 mm diameter) quartz ampoule. The ampoule, containing 1.5 g of the mixture, was evacuated to a pressure of 10^{-5} Torr and sealed. The ampoule was then heated in an electric furnace to a temperature of $310\text{ }^{\circ}\text{C}$ for 5 days. Afterwards its temperature was first raised to $590\text{ }^{\circ}\text{C}$ for 1 day and then to $900\text{ }^{\circ}\text{C}$ for 3 h. At this temperature the ampoule was frequently shaken to ensure good mixing of the melt. The ampoule was then quenched to $0\text{ }^{\circ}\text{C}$ in an ice-water mixture. However, this procedure did not yield the required glasses as was verified from their X-ray diffraction patterns obtained with Cu K_{α} radiation ($\lambda=1.540598\text{ \AA}$). Thus, the substance in the ampoule was obtained, grounded in a glove box, refilled in the quartz ampoule, sealed under vacuum, and transferred to the electric furnace. Then, the temperature of the electric furnace was first raised to $600\text{ }^{\circ}\text{C}$ for 1 h and then to $900\text{ }^{\circ}\text{C}$ at the rate of $100\text{ }^{\circ}\text{C}/\text{h}$. Finally, the quenching was done in an ice-water mixture to obtain the glass. The amorphous nature of the prepared samples was subsequently rechecked by X-ray diffraction. The X-ray patterns of $\text{Ge}_{22}\text{Se}_{72}\text{Fe}_6$, $\text{Ge}_{24}\text{Se}_{70}\text{Fe}_6$ and $\text{Ge}_{27.33}\text{Se}_{66.67}\text{Fe}_6$ are shown in Fig.1. The X-ray diffraction pattern of $\text{Ge}_{27.33}\text{Se}_{66.67}\text{Fe}_6$ (bottom curve) indicates that it is a partly crystalline sample and therefore its results and the results of the samples with similar X-ray patterns are not included in the data analysis.

The glass transition and onset crystallization temperatures for Ge-Se-Fe glasses were measured by means of differential scanning calorimetry using Netzsch DSC 404C calorimeter. The heating rate employed was $10\text{K}/\text{min}$. The samples with masses ranging between 50-75 mg were measured in evacuated silica tubes (length=15 mm; diameter= 6.3 mm; wall thickness=0.4 mm) with an empty silica tube serving as a reference. The calorimeter was calibrated in temperature with the melting points of Ga, In, Pb, Sb and Zn. The melting temperatures were measured using DTA instrument equipped with Ni/Cr Ni

thermocouples. The system was calibrated with the melting points of Ga, In, Pb, Sb and Ag. The samples, with masses between 50 and 60 mg, were sealed in evacuated silica tubes (length= 35 mm; diameter 4.0 mm; wall thickness= 0.5 mm) and referenced to an empty silica tube. The scans were done with a heating rate of 10 K/min.

3. Results and discussion

The average coordination number, n , of the studied glasses is evaluated using the standard procedure [9] which requires the knowledge of the coordinations of the elements constituting the glassy alloy. Coordinations of 4 for Ge and 2 for Se, conforming with the well-known Mott's (8-N) rule [10] with N being the number of outer shell electrons, have been used in the calculation of n . Because of the lack of any direct structural determination of the coordination number of Fe in these glasses, and as in previous investigations [8,11,12], a value of 2 for its coordination has been used. For $\text{Ge}_x\text{Se}_{100-x-y}\text{Fe}_y$ the average coordination number, n , is given by

$$n=2+0.02x \quad (1)$$

where x is the atomic concentration of Ge in the glassy alloy. The calculated values of n for the prepared glasses are given in table 1.

The DSC results show that the as-prepared glasses exhibit a glass transition upon heating and, depending on their composition, an exothermic crystallization peak (or absence of it). The measured characteristic temperatures, T_g and T_c , of the investigated glasses are listed in table 1. The T_g values range from 314-583, 356-549, and 345-560 K for glasses containing 2, 4, and 6 at % Fe, respectively. For the samples which showed crystallization effects, the values of their T_c cover a range from 374-668, 631-647, and 389-663 K, respectively, for glasses containing 2, 4, and 6 at % Fe. The melting points, T_m , determined from DTA, range between 1071-1079 K for Fe_2 , 1074-1101 K for Fe_4 , and 1075-1122 K for Fe_6 families of the prepared glasses and are also listed in table 1. From the characteristic temperatures, the glass thermal stability has been estimated using Dietzel $\Delta T = T_c - T_g$ criterion

[13]. According to this criterion, the kinetic resistance to crystallization increases with increasing ΔT . Thus, this temperature interval gives an indication of the thermal stability of the glass [14, 15] wherein a small ΔT signifies that the glass contains structural units with a high crystallization tendency and vice versa. As it can be seen from table 1 and Fig. 2, the glassy alloys with the chemical compositions $\text{Ge}_{20}\text{Se}_{78}\text{Fe}_2$, $\text{Ge}_{20}\text{Se}_{76}\text{Fe}_4$ and $\text{Ge}_{20}\text{Se}_{74}\text{Fe}_6$ and all having the same coordination number of 2.40, are the most stable ones with the maximum ΔT interval. Another parameter usually employed to estimate the glass thermal stability is the one introduced by Hruby, H_r [16], and defined as follows :

$$H_r = \Delta T / (T_m - T_c) \quad (2)$$

Regarding T_g as the temperature at which the supercooled liquid solidifies to a glass, this H_r parameter accentuates the fact that the probability of obtaining a glass increases as the supercooling temperature ($T_m - T_c$) decreases and ΔT increases. If $H_r \leq 0.1$, the glass is usually difficult to prepare and good glass formers normally have values of $H_r \geq 0.4$. It may be noted that the H_r values of Ge-Se-Fe glasses, given in table 1, demonstrate that these glasses can be classified among those which are difficult to prepare. This might explain the scarcity of studies on glasses of this system. Furthermore, the value of H_r presents a maximum (see table 1 and Fig. 3) for compositions having an average coordination number of 2.40, thus following the same pattern as ΔT . This unequivocally manifests that glasses having $n=2.40$ are the most stable ones.

The observed maxima in ΔT and H_r can be understood on the basis of Phillips'-Thorpe constraint theory proposed for covalently bonded glasses [17-21]. To explain the strong glass- forming ability of network alloy compositions, and according to this theory, where only short-range order structures are considered, the number of degrees of freedom in a covalently bonded glass, N_d , exhausts the number of constraints due to bond stretching, $N_{c\alpha}$, and bond bending, $N_{c\beta}$, .The balance condition $N_c = N_d$, where $N_c = N_{c\alpha} + N_{c\beta}$, led Phillips to conclude that the stability for the network with the critical coordination number $n=2.40$ is

optimised. The same result was arrived at by Thorpe [19] by counting the number of zero-frequency modes. He showed that for a network embedded in 3-dimensional space, the number of zero frequency modes per atom, f , is given by

$$f=2-\frac{5}{6}n \quad (3)$$

which approaches zero as n approaches 2.40 from below. Thus, at this critical coordination number there is a transformation from underconstrained floppy network to overconstrained rigid network and the network attains its maximum stability. The present observations of maxima in ΔT and H_r at $n=2.40$ are, thus, a realization of Phillips'-Thorpe threshold in Ge-Se-Fe glassy alloys. Ample experimental evidence in support of the existence of this threshold in the property-composition dependence for chalcogenide glasses comes from thermal [22-24], neutron [25,26], Mossbauer [27-30], mechanical [31], electronic [32], vibrational [33-35], and physicochemical [22, 24] measurements. Furthermore, its existence has been confirmed by computer simulations of bond-depleted diamond network [36], 2D triangular central force networks [37], and self-organising networks [38]. In addition to the above observations, it is interesting to note from Fig. 4 that the average coordination number dependence of the glass transition, even when T_g is examined in totality for all three studied glassy families, is linear. This is in accordance with the modified Gibbs-DiMarzio equation [39] given by

$$T_g = \frac{T_0}{1-\beta(n-2)} \quad (4)$$

where T_0 is the glass transition temperature of the non-cross-linked initial polymeric chain, β is a system parameter and n is the average coordination number. In the high chalcogen limit, equation (4) can be expressed as

$$T_g \cong T_0[1+\beta(n-2)] \quad (5)$$

which is linear if T_g is plotted versus n , as observed. The absence of extrema in the T_g - n dependence when the average coordination number reaches the critical value of 2.40 has also been reported in other glassy selenide systems [40-42].

For many chalcogenide systems a linear correlation between the glass transition temperature with the overall mean bond energy of the covalent glassy network $\langle E \rangle$ is observed [43, 45]. To test the validity of this correlation for Ge-Se-Fe system, we have calculated $\langle E \rangle$ for the investigated glassy alloys. This is done by using the covalent bond approach (CBA) [43]. In CBA, the mean bond energy of the average cross-linking per atom, $\langle E_c \rangle$, in $\text{Ge}_A\text{Fe}_B\text{Se}_C$ glasses, in the chalcogen-rich region, as in our case, is given by

$$\langle E_c \rangle = 4A E_{Ge-Se} + 2B E_{Fe-Se} \quad (6)$$

where A, 4, B and 2 correspond, respectively, to the atomic concentration and coordination number of Ge and Fe atoms. The heteropolar bond energies for Ge-Se and Fe-Se have been calculated from Pauling [44] using the relation

$$E_{a-b} = 0.5(E_{a-a} + E_{b-b}) + 23(X_a - X_b)^2 \quad (7)$$

where X_a , X_b , E_{a-a} and E_{b-b} correspond to the electronegativity and homopolar bond energy of a and b atoms, respectively. Next, the average bond energy per atom of the ‘remaining matrix’, $\langle E_{rm} \rangle$, is defined as:

$$\langle E_{rm} \rangle = \frac{2\left(\frac{n}{2} - 4A - 2B\right)E_{Se-Se}}{n} \quad (8)$$

Finally, $\langle E \rangle$ is the sum of the two contributions and given by

$$\langle E \rangle = \langle E_c \rangle + \langle E_{rm} \rangle \quad (9)$$

Thus, $\langle E \rangle$ is determined by the degree of cross-linking, the bond energy, the average coordination number, and the bond type. It is also known that all these factors influence the T_g of the glass network [43].

The calculated values of $\langle E \rangle$ are listed in table 1. As it is seen from this table, $\langle E \rangle$ increases with increasing n, thus following the same trend as T_g for this glassy system. Furthermore, a plot of T_g versus $\langle E \rangle$ in these glasses, depicted in Fig. 5, shows a linear

dependence. A highly significant correlation between T_g and $\langle E \rangle$, in units of kcal/mole, of the form

$$T_g = -427 + 17.4 \langle E \rangle \quad (10)$$

is obtained, where a least squares line has been fitted to the calculated data. This system, therefore, is found to respect the reported linear T_g - $\langle E \rangle$ behaviour obtained for many chalcogenide glassy materials at the high chalcogen content. The explanation of the origin of T_g and the correlation of T_g with other physical and chemical properties of glasses reveals that T_g is related to the rigidity of the glass network [43]. This rigidity is usually associated with the average coordination number which is a measure of the overall mean bond energy between atoms or entities of a glass. Because a linear correlation between T_g and the average coordination number is observed, one would expect T_g to scale linearly with $\langle E \rangle$, as obtained.

4. Conclusions

The thermal stability of Ge-Se-Fe glasses has been studied using differential scanning calorimetry and differential thermal analysis measurements. The obtained results reveal that the thermal stability of the three families of the investigated glassy alloys, as inferred from ΔT and H_r parameters, attains a maximum at the average coordination number $n=2.40$. This observation is a realization of Phillips'-Thorpe percolation threshold where the maximum stability of the network is just obtained if this percolation threshold limit is reached. The overall bond energies of the studied glasses have also been calculated using the CBA. The dependence of T_g on $\langle E \rangle$ is found to be linear which is in agreement with recently reported results [45].

Acknowledgements

One of us, G.Saffarini., gratefully acknowledges the financial support from the Arab Fund for Economic and Social Development, Kuwait

References

- [1] J. Rowlands, S. Kasap, *Phys. Today* 50 (1997) 24.
- [2] D.P. Machewirth, K. Wei, V. Krasteva, R. Datta, E. Snitzer, G.H. Siegel, *J. Non-Cryst. Solids* 213-214 (1997) 295.
- [3] K. Tanaka, *Curr. Opin. Solid State Mater. Sci.* 1 (1996) 567.
- [4] J.S. Sanghera, F.H. Kung, L.E. Busse, P.C. Pureza, I.D. Aggarwal, *J. Am. Ceram. Soc.* 78 (1995) 2198.
- [5] K. Wei, D.P. Machewirth, J. Wenzel, E. Snitzer, G.H. Sigel, *J. Non-Cryst. Solids* 182 (1995) 257.
- [6] S.Kasap, in: A.S. Diamond (Ed.), *Handbook of Imaging Materials*, Marcel Dekker, New York, 1991, p.329.
- [7] P. Boolchand, W.J. Bresser, *Nature* 40 (2001) 1070.
- [8] Z.G. Ivanova, V.S. Vassilev, *J. Phys. Chem. Solids* 58 (1997) 1347.
- [9] S.R. Elliot, *Physics of Amorphous Materials*, Longmann, London, 1990, p.61.
- [10] N.F. Mott, *Philos. Mag.* 19 (1969) 835.
- [11] G. Saffarini, J. Matthiesen, *Appl. Phys. A* 73 (2001) 621.
- [12] G.Saffarini, J. Matthiesen, R. Blachnik, *Physica B* 305 (2001) 293.
- [13] A. Dietzel, *Glasstech. Ber.* 22 (1968) 1187.
- [14] K.L. Bhatia, S.C. Katyal, A.K. Sharma, *J. Non-Cryst. Solids* 58 (1983) 27.
- [15] S. Mahadevan, A. Giridhar, A.K. Singh, *J. Non-Cryst. Solids* 88 (1986) 11.
- [16] A. Hruby, Czech, *J. Phys. B* 22 (1972) 187.
- [17] J. C. Phillips, *J. Non-Cryst. Solids* 34 (1979) 153.
- [18] J. C. Phillips, M.F. Thorpe, *Solid State Commun.* 53 (1985) 699.
- [19] M.F. Thorpe, *J. Non-Cryst. Solids* 57 (1983) 355.
- [20] H. He, M.F. Thorpe, *Phys. Rev. Lett.* 54 (1985) 2107.
- [21] M.F. Thorpe, *J. Non-Cryst. Solids* 182 (1995) 135.

- [22] U. Senapati, A.K. Varshneya, *J. Non-Cryst. Solids* 185 (1995) 289.
- [23] M. Tatsumisaga, B.L. Halfpap, J.L. Green, S.M. Lindsay, C.A. Angell, *Phys. Rev. Lett.* 64 (1990) 1549.
- [24] A. Feltz, H. Aust, A. Blayer, *J. Non-Cryst. Solids* 55 (1983) 179.
- [25] W.A. Kamitakahara, R.L. Cappelletti, P. Boolchand, B. Halfpap, F. Gompf, D.A. Neumann, H. Mutka, *Phys. Rev. B* 44 (1991) 94.
- [26] P. Boolchand, R.N.ENZWEILER, R.L. Cappelletti, W.A. Kamitakahara, Y. Cai, M.F. Thorpe, *Solid State Ionics* 39 (1990) 81.
- [27] B. Norban, D. Persing, R.N.ENZWEILER, P. Boolchand, J.E. Griffiths, J.C. Phillips, *Phys. Rev. B* 36 (1987) 8109.
- [28] W. Bresser, P. Boolchand, P. Suranyi, *Phys. Rev. Lett.* 56 (1986) 2493.
- [29] M. Zhang, P. Boolchand, *Science* 266 (1994) 1355.
- [30] P. Boolchand, W. Bresser, M. Zhang, Y. Wu, J. Wells, R.N.ENZWEILER, *J. Non-Cryst. Solids* 182 (1995) 143.
- [31] R. Bohmer, C.A. Angell, *Phys. Rev. B* 45 (1992) 10091.
- [32] S. Asokan, G. Parthasarathy, E.S.R. Gopal, *Philos. Mag. B* 57 (1988) 49.
- [33] X. Feng, W. Bresser, P. Boolchand, *Phys. Rev. Lett.* 78 (1997) 4422.
- [34] B. Uebbing, A.J. Sievers, *Phys. Rev. Lett.* 76 (1996) 932.
- [35] J.C. Phillips, *Phys. Rev. B* 54 (1996) R6807.
- [36] D.S. Franzblau, J. Tersoff, *Phys. Rev. Lett.* 68 (1992) 2172.
- [37] D.J. Jacobs, M.F. Thorpe, *Phys. Rev. Lett.* 75 (1995) 4051.
- [38] M.F. Thorpe, D.J. Jacobs, M.V. Chubyns, J.C. Phillips, *J. Non-Cryst. Solids* 266-269 (2000) 859.
- [39] A.N. Sreeram, D.R. Swiler, A.K. Varshneya, *J. Non-Cryst. Solids* 127 (1991) 287.
- [40] S. Asokan, M.V.N. Prasad, G. Parthasarathy, E.S.R. Gopal, *Phys. Rev. Lett.* 62 (1989) 808.

- [41] S. Mahadevan, A. Giridhar, *J. Non-Cryst. Solids* 151 (1992) 245.
- [42] S. Mahadevan, A. Giridhar, *J. Non-Cryst. Solids* 152 (1993) 42.
- [43] L. Tichy, H. Ticha, *J. Non-Cryst. Solids* 189 (1995) 141.
- [44] L. Pauling, *Die Nature der Chemischen Bindung*, VCH, Weinheim, 1976, pp. 80-89.
- [45] M. Micoulaut, *C.R. Chimie* 5 (2002) 825.

Captions

Table 1: Glass compositions; calculated values of the average coordination number; measured glass transition, crystallization and melting temperatures; Dietzel temperature interval; Hruby parameter and calculated overall mean bond energies.

Fig. 1: Typical X-ray diffraction patterns obtained from the compositions $\text{Ge}_{22}\text{Se}_{72}\text{Fe}_6$ (top curve), $\text{Ge}_{24}\text{Se}_{70}\text{Fe}_6$ (middle curve), and $\text{Ge}_{27.33}\text{Se}_{66.67}\text{Fe}_6$ (bottom curve).

Fig. 2: The variation of Dietzel temperature interval with the average coordination number for glassy compositions containing 2 at % Fe (squares), 4 at % Fe (circles) and 6 at % Fe (triangles). The solid lines drawn are a mere connection of the data points to guide the eye.

Fig. 3: The variation of Hruby parameter with the average coordination number for glassy compositions containing 2 at % Fe (squares), 4 at % Fe (circles) and 6 at % Fe (triangles). The solid lines drawn are a mere connection of the data points to guide the eye.

Fig. 4: The dependence of the glass transition temperature of all studied glass families on the average coordination number.

Fig. 5: The dependence of the glass transition temperature of all studied glass families on the overall mean bond energy.

Table 1

Glass composition Ge Se Fe	n	T_g (K)	T_c (K)	T_m (K)	ΔT	H_r	<E > (kcal/mole)
0 98 2	2.0	314	374	1071	60	0.086	43.84
4 94 2	2.08	353	453	1081	100	0.159	44.74
8 90 2	2.16	369	No exo.	1079	-	-	46.13
12 86 2	2.24	393	No exo.	1082	-	-	47.97
18 80 2	2.36	448	641	1095	193	0.425	51.46
20 78 2	2.40	486	736	1100	250	0.687	52.80
22 76 2	2.44	525	644	1108	119	0.257	54.22
24 74 2	2.48	546	645	1111	99	0.213	55.72
28 70 2	2.56	583	668	1079	85	0.207	58.92
2 94 4	2.04	356	No exo	1074	-	-	44.09
6 90 4	2.12	369	No exo	1084	-	-	45.31
10 86 4	2.20	393	No exo.	1087	-	-	46.99
14 82 4	2.28	431	No exo.	1082	-	-	49.09
18 78 4	2.36	488	631	1096	143	0.308	51.56
20 76 4	2.40	479	632	1104	153	0.324	52.93
22 74 4	2.44	519	632	1104	113	0.239	54.37
24 72 4	2.48	549	647	1101	98	0.216	55.89
2 92 6	2.04	345	No exo.	1075	-	-	43.96
6 88 6	2.12	357	389	1077	32	0.047	45.25
10 84 6	2.20	395	No exo.	1083	-	-	46.99
14 80 6	2.28	422	No exo.	1089	-	-	49.14
18 76 6	2.36	477	576	1097	99	0.190	51.67
20 74 6	2.40	492	637	1106	145	0.309	53.06
22 72 6	2.44	531	639	1117	108	0.226	54.52
24 70 6	2.48	560	663	1122	103	0.224	56.07

Fig. 1

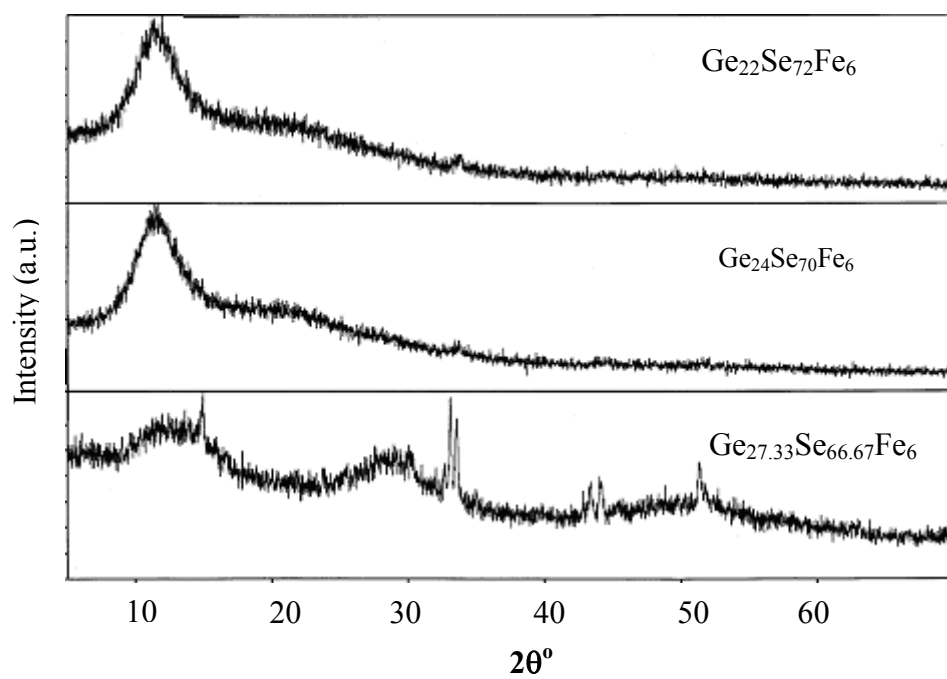


Fig.2

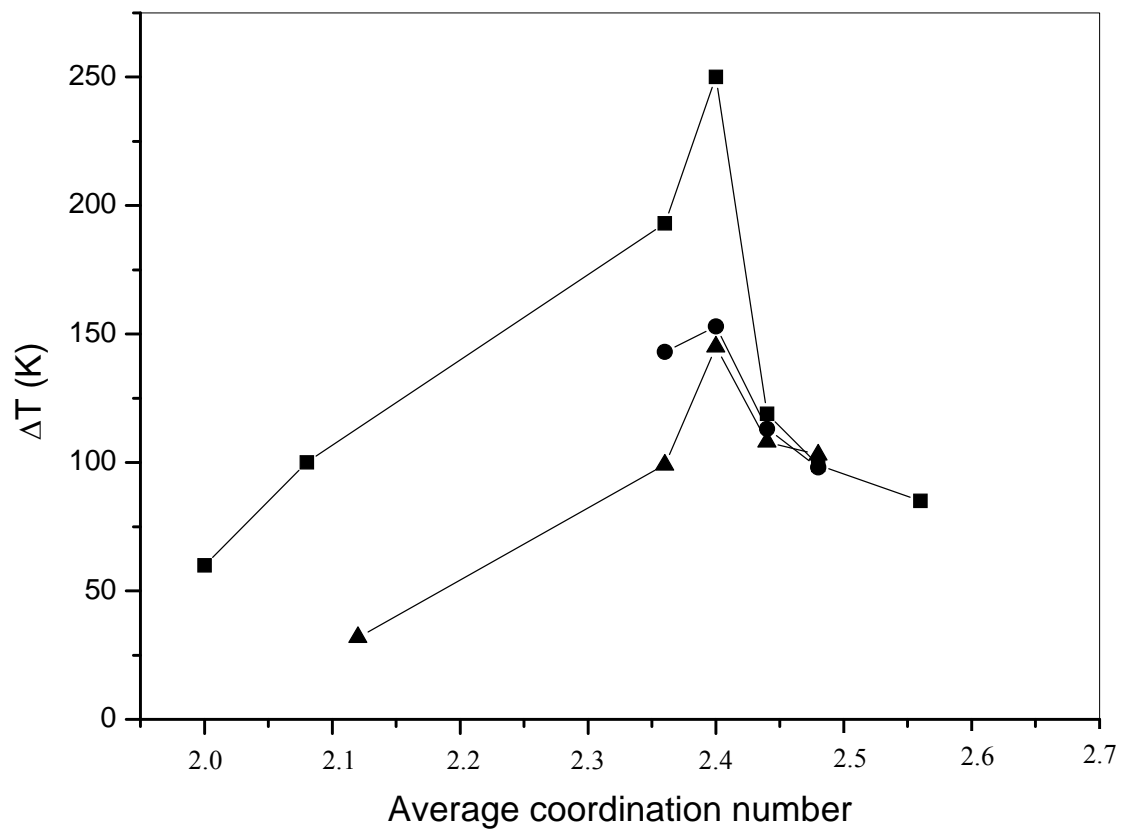


Fig.3

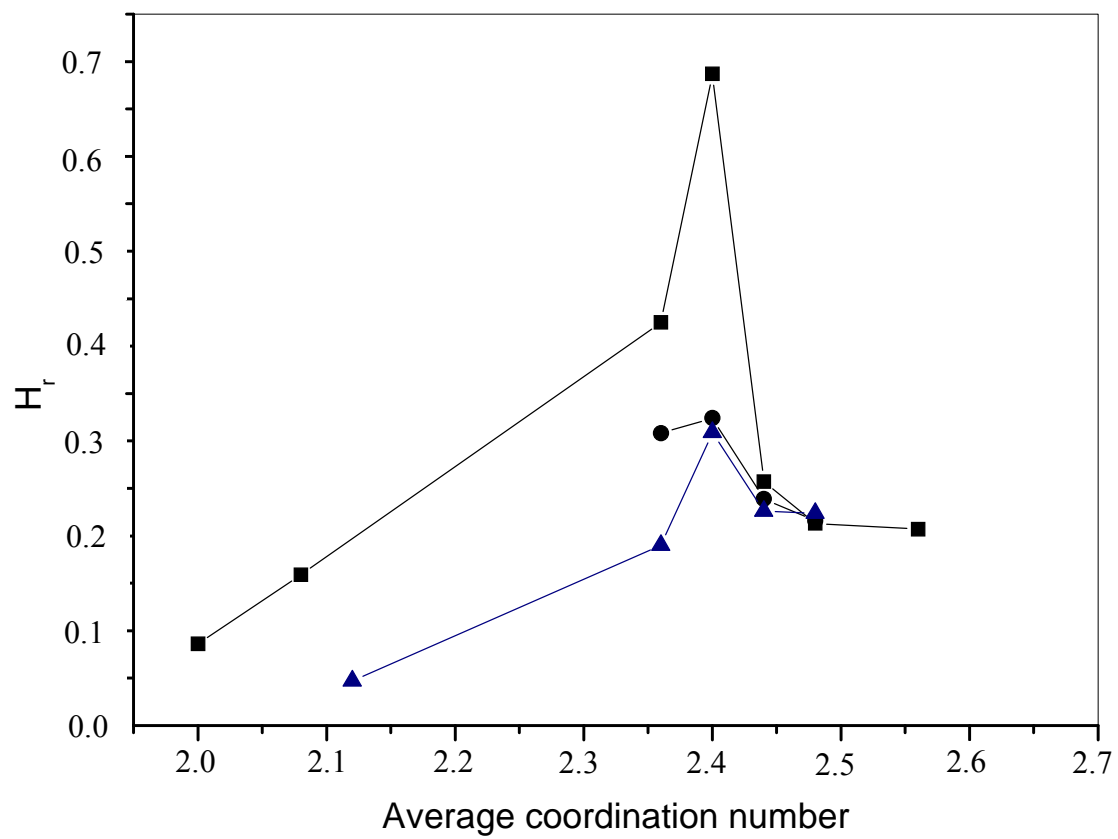


Fig.4

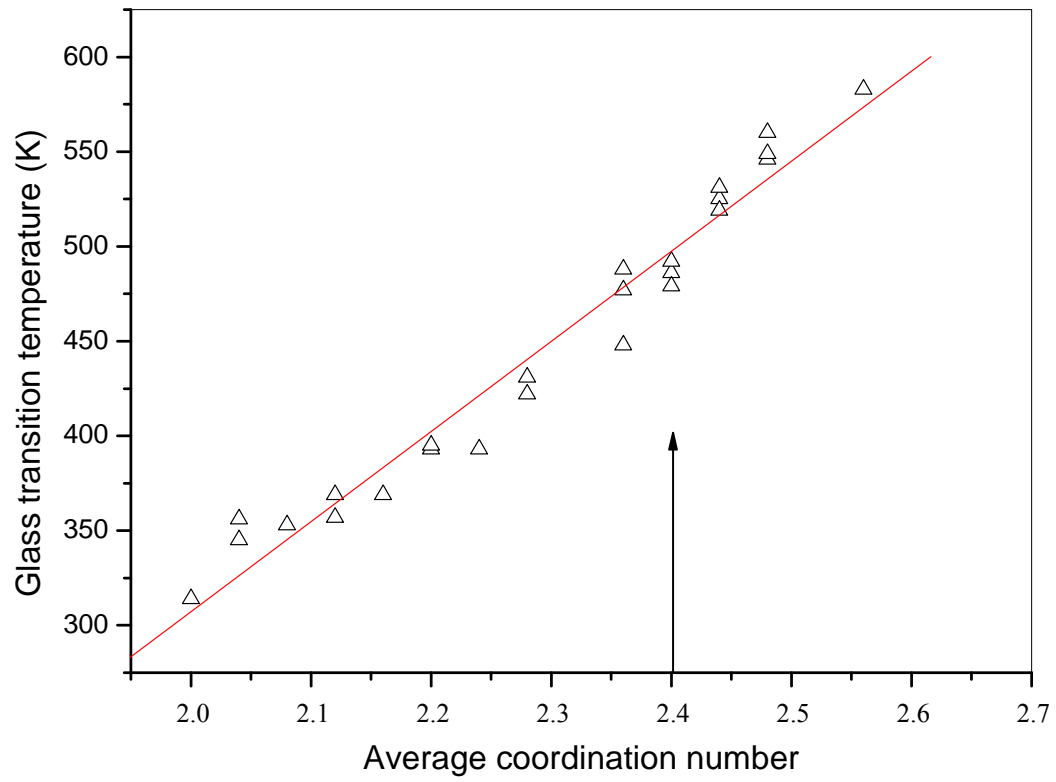


Fig.5

